Overview of the D3R Observations During the ICE-POP Field Campaign With Emphasis on Snow Studies

Shashank S. Joshil, *Student Member, IEEE*, V. Chandrasekar, *Fellow, IEEE*, and David B. Wolff

***Abstract*—The International Collaborative Experiment during the PyeongChang Olympics and Paralympic winter games 2018 took place in the PyeongChang region of South Korea. The main goal of this field campaign was to study winter precipitation in an environment that has complex terrain. The NASA dual-frequency, dual-polarization, Doppler radar (D3R) was calibrated and deployed in this field campaign. The positioning error of the radar was calibrated to be within 0.1°. The D3R was deployed for more than four months and was able to capture many interesting snowfall events along with a few rain events. In this article, the deployment and performance of the D3R during the campaign are discussed. The snowfall events captured by the D3R are discussed in detail to interpret the microphysics from a radar's perspective. The reflectivity–snowfall rate relationship is derived at the Ku band, and the snow accumulation computed is in good agreement with a precipitation gauge that was deployed near the radar. The benefit of the dual-frequency ratio for identifying the precipitation particle types is briefly introduced using the data from a large snow event on 28th February 2018. The vertical profile D3R data for this snow event are studied for detecting the presence of pristine-oriented ice crystals in the mixed hydrometeor phase conditions. Various other instruments, such as X-band radar and disdrometers, were deployed in the campaign. The D3R data are compared with the MxPOL X-band radar, and the reflectivity values match within a couple of dB in the common volume region.**

***Index Terms*—Dual-frequency, dual-polarization, Doppler radar (D3R), International Collaborative Experiment during the PyeongChang Olympics and Paralympic winter games (ICE-POP), instruments, Ku-band, snow, weather radar.**

I. Introduction

IN EARLY 2018, the PyeongChang region in South Korea hosted the International Collaborative Experiment during the PyeongChang Olympics and Paralympic winter games (ICE-POP) field campaign. Since the Olympics and Paralympics games require significant precipitation on the ground, the campaign was scheduled in the winter season of South Korea. Many active and passive remote sensing instruments were deployed in this field campaign. The primary goal of the ICE-POP 2018 campaign was to understand the winter precipitation regime in the PyeongChang region, which has a complex terrain, and the associated processes, with the focus on improving the short-term forecasting and nowcasting systems [1]. The PyeongChang region encounters a huge amount of snowfall and records very low temperatures in the winter season. In addition, since the coastline of the ocean is near this region, the observations during this campaign will aid in understanding the climate interactions between ocean and mountain regions and the formation of clouds and snow [2]. The remote sensing observations captured by various instruments will aid in understanding the microphysics of the snow clouds and the evolution of the weather events spatially and temporally. The Korean Meteorological Administration (KMA) and the National Institute of Meteorological Science supported the ICE-POP field campaign.

Remote sensing observations are widely used to understand the microphysical process happening within precipitation events. In the past, radars have shown their usefulness and potential for studying microphysical processes. While instruments such as disdrometers, multiangle snowflake cameras, and particle imaging probes are useful in getting the point measurements, scanning weather radars can collect precipitation data over a wide area. The maximum unambiguous range for a typical X-band radar is around 40–60 km.

Radars can be used to understand the evolution and progress of the storms. Since the operating frequency of the radar limits the minimum precipitation particle size that can be observed, the sensitivity of observing smaller precipitation particles increases with frequency. Since the size of the snow particles is small compared to rain particles, high-frequency radars above 10 GHz are suitable for studying snow and interpreting the mixed-phase precipitation conditions. The combination of remote sensing observations from different instruments, such as radars and disdrometers, will aid in understanding the precipitation process in detail.

The NASA dual-frequency, dual-polarization, Doppler radar (D3R) [3], [4] was initially developed to support ground validation (GV) operations of the global precipitation measurement (GPM) mission [5]. The D3R operates at the high-frequency bands of Ku (13.9 GHz) and Ka (35.5 GHz). These frequency bands of the D3R radar are the same in which the GPM's

Manuscript received 12 July 2022; revised 3 September 2022, 18 November 2022, and 28 December 2022; accepted 20 January 2023. Date of publication 24 January 2023; date of current version 6 February 2023. This work was supported by the NASA GPM Ground Validation Program. *(Corresponding author: Shashank S. Joshil.)*

Shashank S. Joshil and V. Chandrasekar are with the Colorado State University, Fort Collins, CO 80523 USA (e-mail: sjoshil@colostate.edu; chandra@colostate.edu).

David B. Wolff is with the NASA Wallops Flight Facility, Wallops Island, VA 23337 USA (e-mail: david.b.wolff@nasa.gov).

Digital Object Identifier 10.1109/JSTARS.2023.3239593

Fig. 1. NASA D3R deployed on the rooftop of DGW during the ICE-POP field campaign in South Korea.

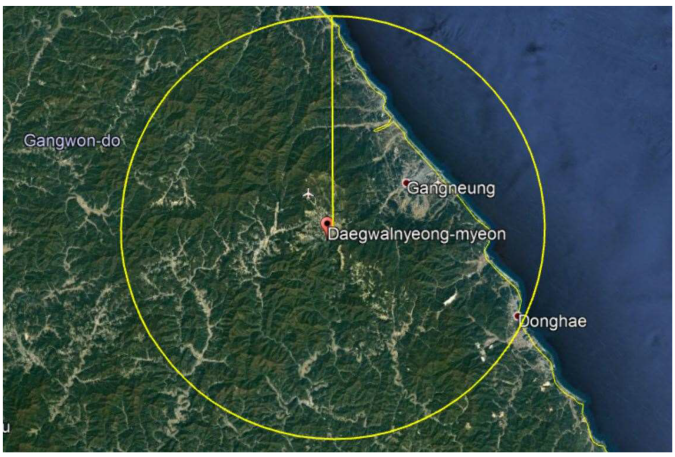

Fig. 2. Maximum unambiguous range of D3R during ICE-POP campaign.

dual-frequency precipitation radar operates, which aids in comparisons from satellite and ground observations. The D3R was deployed in various field campaigns across North America under a variety of warm and cool season conditions and collected good-quality data [6]. In the past, a notable campaign in which the D3R collected winter precipitation data was the GCPEx field campaign in Ontario, Canada. The data collected during this campaign aided various researchers in improved understanding of microphysics. As such, the D3R was an ideal candidate for the ICE-POP field campaign to collect winter precipitation data.

The NASA D3R was stationed at Wallops Flight Facility, Virginia, USA, before the ICE-POP deployment. The D3R was disassembled and shipped to South Korea in late August 2017, and the assembly of the D3R in South Korea was done in late October 2017. The D3R was deployed on the rooftop of the Daegwallyeong regional weather office (DGW) in the PyeongChang province of South Korea for the ICE-POP field campaign. This location was situated very close to the main stadium of the Winter Olympics, where many sporting events were held. Fig. 1 shows the D3R in operation on top of the DGW during one of the campaign days. The maximum unambiguous operating range of the D3R is 40 km, as shown in Fig. 2. The mountains and coastal regions around the D3R can also be seen in this picture. The D3R will aid in understanding the evolution of the snow clouds through its Doppler velocity and dual polarization observations. Since the D3R was deployed in mountainous terrain, as shown in Fig. 2, there were radar beam blockages at lower elevation angles. At 0.5° elevation, the radar plan position indicator (PPI) scan coverage was only 5%. At 3° and 5° elevations, the radar PPI scan coverage was 52% and 89%, respectively. Above 7.5°, the full PPI scan coverage was obtained.

An overview of the snow observations and data collected during ICE-POP is discussed in this article. The article is structured as follows. The D3R calibration and the events captured during the ICE-POP campaign are discussed in Section II. A relationship between the radar moments and the snowfall rate (SR) is obtained, and the results are shown in Section III. The D3R data to interpret some of the snow microphysical processes are explained in Section IV with the help of vertical profile analysis and hydrometeor classification. The potential of using dual-frequency ratio (DFR) for studying microphysics is briefly discussed in Section V. Section VI gives a brief discussion of other instruments that were deployed in the campaign and the potential of combining their data with D3R data to enhance the understanding of winter precipitation. Finally, a summary is given in Section VII.

II. D3R Calibration and Events Captured During ICE-POP Field Campaign

Before the deployment to the ICE-POP campaign in South Korea, the D3R went through system upgrades until early 2017. Some of the subsystems were redesigned and upgraded to enhance the radar observing capabilities. Prior to the deployment of the D3R radar, system parameters were well calibrated using various calibration methods. One of the calibration methods used for adjusting the gain and the received power levels is the calibration using a corner reflector. The radar was calibrated using a corner reflector with known dimensions placed on top of a tower located at a predefined distance from the radar [7]. The corner reflector is adjusted such that the maximum power return is received. The radar system parameters are then adjusted by comparing the return power levels with the theoretical power level return expected. This ensures that correct return power values are received, and optimal performance is achieved from the radar. The uncertainty in received power when using the corner reflector for calibration is within 0.5 dB. More details on the corner reflector calibration can be found in [8] and [9]. To verify the accuracy of the radar moments, the D3R data were cross validated with data from another radar. A nearby U.S. National Weather Service radar S-band radar was used for the cross validation. The data analysis showed a good match between the radar moments [10]. Both corner reflector calibration and validation were done prior to the shipment of the D3R radar for the ICE-POP campaign.

As mentioned earlier, the D3R radar was deployed in DGW for the campaign in late October 2017. Deploying the radar well in advance for the ICE-POP campaign helped in calibrating the

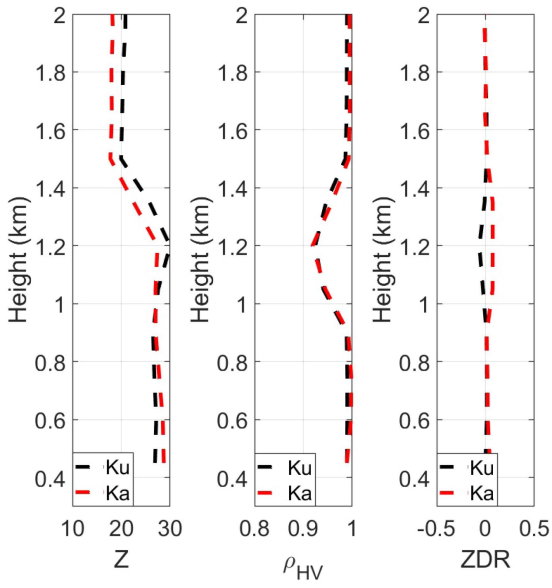

Fig. 3. Birdbath scan data collected on 10th of November 2017 at 07:32 UTC (left to right) reflectivity, co-pol correlation, and differential reflectivity.

system accurately and capturing some early rain events to ensure the system was performing well. Periodic solar calibration was done during the ICE-POP field campaign. The solar calibration exercise is a routine calibration process for the D3R, which is used to align and adjust the antenna offset between the Ku and Ka band radars. Solar calibration is also used to determine the azimuth offset of the radar with respect to the true north, and this is done with the information of the sun's position. The position of the sun is known for a particular location and time during the day. The radar is scanned around the sun's position, and the offset in azimuth is then determined. If the position of the sun and the radar pointing angle is the same, then there will be zero offset. This calibration procedure ensures that the radar is looking at the correct resolution volume when scanning. A slight mismatch of a few degrees offset in azimuth will yield a huge error in the scanning radar resolution volume. A more detailed description of solar calibration is given in [9]. From the solar calibration results, it was seen that there was a very good alignment with azimuth and elevation. The error was within 0.1° in elevation and azimuth.

Periodic checks for the radar systems were carried out to ensure the radar was well calibrated. Postprocessing of D3R data from the campaign was also done to ensure the bias in differential reflectivity was accounted for and corrected. Fig. 3 shows data from a birdbath scan in light rain collected on the 10th of November 2017 at 07:32 UTC. From this figure, it can be seen that the radar variables, differential reflectivity, and co-polar correlation between Ku and Ka bands are in good agreement. There is a drop in co-polar correlation, and a knee-shaped reflectivity profile can be seen around 1.2 km in height. This corresponds to the melting layer present at that height. The differential reflectivity is around 0 dB below the melting layer, which is expected for data captured in light rain conditions when pointing vertically [11]. The value of the co-polar correlation from the surface up to about 0.9 km is close to 1 for both Ku and Ka, which is expected as the hydrometeor particle type is the same within the resolution volumes. In the region corresponding to the melting layer, the co-polar correlation falls to very low values. As a result, the agreement between the Ku and Ka data will have a higher standard deviation. Because of this, we see a small difference in differential reflectivity values in this region. It can be noticed that the reflectivity of the Ku data is higher than the Ka data, which can be observed clearly above the melting layer. This is due to the large signal attenuation encountered at Ka band compared to the Ku band.

The D3R radar is capable of performing multiple scan strategies such as PPI scan, range height indicator (RHI) scan, fixed pointing scan, and birdbath scan. The birdbath scan is a vertically pointing (90° elevation) full azimuth rotation scan. There is flexibility in D3R's user interface software which allows the radar operator to set up the scan strategy according to the needs and can combine different types of scans sequentially. The change in scan strategy can be accomplished with ease within a couple of minutes using the graphical user interface (GUI) of the D3R radar. The GUI of the radar also displays real-time images of the scans captured by the radar. The radar scan images that were generated were also sent to the KMA display so that the forecasters monitoring the weather conditions could use the data from the radar to make decisions accordingly. The data from D3R helped the forecasters monitor snow conditions on the opening day of the Winter Olympics, which could not be detected by other radars present in the KMA network.

III. Snowfall Rate Estimations

The SR estimations provide information on the amount of snow accumulation during the precipitation event. Accurate estimates of SR play a significant role in various hydrological and meteorological models. Instruments, such as Parsivel disdrometers, 2-D video disdrometer, and precipitation gauges which were deployed in the ICE-POP campaign, were used to measure the snowfall accumulation. Some of these instruments also provide microphysical information about the hydrometeors, such as particle size distribution. However, these instruments have a limitation that they can only provide point measurements and provide accumulation values at the location of the instrument. On the other hand, weather radars provide data over a large area. This is an advantage because the snow accumulation can be mapped over a large area. It should be noted that the resolution of SR and snow accumulation from the radar is limited to the radar's resolution volume. For D3R, the range resolution of the radar was 150 m; estimates are obtained at every 150 m interval. Previously, various quantitative precipitation estimation (QPE) algorithms have been developed. They use the data from point measurement instruments, such as disdrometer as well as radar measurements, to accurately estimate the amount of precipitation received.

In the past, many researchers have come up with a power-law relationship to estimate SRs using radar reflectivity.

However, these relationships were obtained based on the data considered in a particular climatology that was used in their

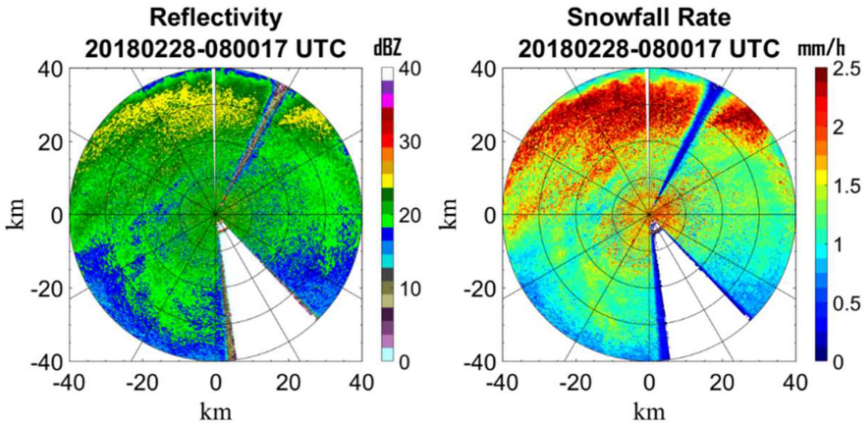

Fig. 4. Reflectivity and SR plots for D3R Ku data taken during a snow event on 28th of February 2018 at 08:00 UTC.

study. The parameters of the snow particles, such as density and mass, vary based on the region. The SR relationships estimated using density determined in [12], [13], and [14] would yield incorrect SR estimates for the events captured in the ICE-POP campaign. Therefore, a new relationship has to be derived for this campaign. Data from the disdrometers deployed in the campaign were used to derive an equation for the estimation of the SR. The density of snow is one of the factors which should be carefully studied as it depends on many factors, such as the type of snow particle and climatology. For accurately estimating the SR for the snow events captured in the campaign, the density of the snow particles was computed using the information of terminal velocity and diameter of the hydrometeor particles measured by the disdrometer. More details on computing the density for the snow events can be found in [15]. Once the density was determined, the SR was obtained, and then the relationship between the SR and reflectivity was determined using the Parsivel disdrometer dataset.

The data considered for obtaining the SR and reflectivity relationship are from a Parsivel disdrometer, which was located at YongPyong Cloud Physics Observatory (YPO). The YPO is located 5.7 km away and approximately 233° azimuth from the location of the D3R radar. The microphysical data such as diameter, velocity, and density of the precipitation particles are considered from the disdrometer to compute the SR. The backscattered radar cross sections were obtained using the T-matrix signal simulations. This was used to compute the reflectivity values at the Ku band. A power-law relationship was then determined between the SR and reflectivity computed from the disdrometer data. The relationship is given as

$$\mathrm{SR} = 0.0921\, Z^{0.5809}. \tag{1}$$

The Ku radar reflectivity and SR images for a PPI scan data recorded at 5° elevation angle on the 28th of February 2018 at 08:00 UTC are shown in Fig. 4. The data in the region from 137° to 172° azimuth and from 25° to 30° azimuth were not present due to the radar beam blockage, as explained earlier. From this figure, it can be seen that the snowstorm covered the entire 40 km range of the D3R, and the SR can be estimated using the relationship derived for the entire region from which the QPE can be obtained. Detailed information on the estimation of the SR for the ICE-POP campaign using disdrometers and D3R can be found in [15].

Fig. 5 shows the 10 and 20 min interval snow accumulation computed using D3R Ku data from 08:00 UTC to 16:00 UTC on the 28th of February 2018. Since the snow particles have a lower fall velocity compared to rain particles and snow accumulation does not change rapidly minute by minute, 10 min and 20 min interval accumulations are considered here. The data point for computing the accumulation was at the YPO site, where a precipitation gauge was also installed. The accumulation estimated from the radar agrees well with the precipitation gauge for both 10 min and 20 min accumulations.

IV. Vertical Profile Analysis to Study Microphysics

Obtaining microphysically interesting parameters directly from remote sensing observations is not easy [16]. As mentioned earlier, the operating frequency of the radar influences the capability of observing smaller hydrometeor particles. To effectively study the microphysics of snow and ice hydrometers, it is desirable to use radars that are operating at frequencies higher than X-band. The D3R radar, which operates at Ku and Ka bands, is sensitive to observing ice clouds and winter precipitation containing ice hydrometeors. Another important aspect to consider is the amount of data available for the researchers to study ice hydrometeors is limited because there are very few scanning weather radars available that operate at these frequency bands.

In addition, falling snow can be characterized using the information of dual-polarimetric measurements and their combinations from D3R [12]. Some previous researchers have used this dual-polarization information to understand the microphysics of ice hydrometers [12], [13]. Along with the reflectivity, the information from other dual-polarization radar moments, such as differential reflectivity (Z_{dr}), co-polar correlation (ρ_{hv}), spectral width (σ_v), and specific phase (K_{DP}), can be used to study the ice hydrometeors. Since the co-polar correlation values have very small variability and, in most situations, values vary between 0.9 and 1, variable L, which is related to the co-polar

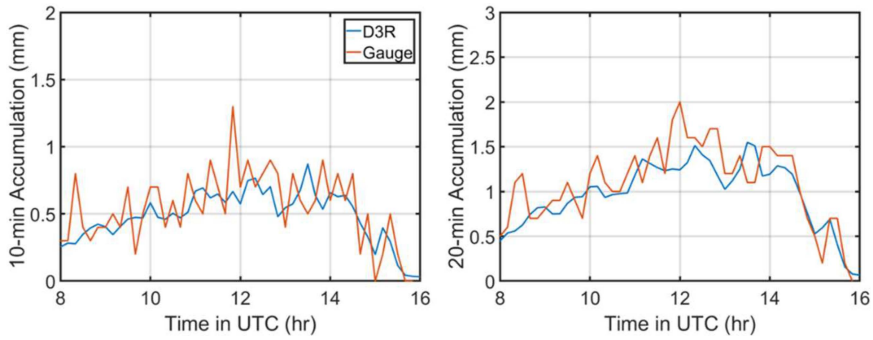

Fig. 5. 10-min (left) and 20-min (right) snow accumulation from D3R and precipitation gauge during a snow event on 28th of February 2018.

correlation, is considered here for the study. The variable L is defined as $L = -\log_{10}(1-\rho_{hv})$, which has a larger range than ρ_{hv} and will be useful in interpreting the values of ρ_{hv}.

A snow case study from the ICE-POP campaign is described in the following. The data are from an RHI scan taken on the 28th of February 2018 at 06:02 UTC. The RHI scans give insight into the vertical structure of the storm event. The D3R was conducting RHI scans along with PPI scans periodically in the campaign. This gives researchers the flexibility to investigate the spatial spread of the precipitation event over the entire unambiguous range covered by the radar, as well as to get the vertical structure of the precipitation event. The snowstorm on the 28th of February 2018 lasted more than 12 h and collected more than 40 cm of snow. The interesting feature of this event was that as the storm progressed, various precipitation phases were observed, such as freezing rain and snow aggregates. The various radar moments for this RHI scan are shown in Fig. 6. It can be seen from this figure that there are interesting features in the various moments, such as a significant increase of differential phase, variations in the spectral width values along the height, and bright band in specific differential phase, which gives information about the precipitation particles.

The use of Z_{dr} and ρ_{hv} to detect the presence of pristine ice crystals along with aggregates was shown in [17]. According to this study, when there is a mixture of pristine ice crystals and aggregates in the radar resolution volume, the Z_{dr} tends to have large values, and the ρ_{hv} will decrease due to the mixture of hydrometeors. Kennedy and Rutledge [18] and Bechini et al. [19] showed that enhanced K_{DP} can be correlated to ice crystal growth in the $-10°$ to $-15°$ temperature range due to vapor deposition. They concluded that the dendritic crystals are most likely causing enhanced K_{DP} to occur between -10 and -18 °C.

From Fig. 6, around 3.6 km in height, a band of enhanced Z_{dr} and relatively low L (i.e., ρ_{hv} close to 1) is observed. This corresponds to the presence of pristine-oriented ice crystals at this height. The K_{DP} values are also enhanced closer to this height, which is expected for pristine ice crystal growth. To further understand the microphysical characteristics of this event, a vertical profile at 8 km from the radar scan is considered. The vertical cut is represented as the dashed black line in Fig. 6. Fig. 7 shows the profile of various radar moments. A temperature profile taken from a sounding instrument on the same day, which was deployed at the site where D3R was present, is also shown in this figure. Since interesting microphysical activity is happening between 0.5 and 5 km in height, the vertical profile is shown only for this region.

From the figures of the vertical profiles considered, we can clearly see that the radar moments and the temperature support the claim of the presence of pristine-oriented ice crystals along with aggregates around 3.6 km in height. The microphysical interpretation for this case is as follows: the nucleation of the pristine-oriented ice crystals starts around 5 km in height. As we go below in height, we can see the Z_{dr} starts to increase and L value starts to decrease. This is because the aggregates are forming among the pristine-ice crystals due to vapor decomposition. At 3.6 km in height, we can see the peak of Z_{dr} and K_{DP} and low value of L. This height can be considered as the height where the pristine ice crystals and aggregate particles achieve a balance with respect to the concentration. The temperature at this height is around -15 °C, which supports the claim of pristine-ice crystals present. Between 3.6 and 3 km, the K_{DP} values further increase, indicating continued growth of pristine ice. The temperature at 3 km is -10 °C supporting pristine crystals can be formed, which is consistent with the previous literature. Below 3 km, both K_{DP} and Z_{dr} decreases and L increases, which indicates aggregates start to grow and increase in number and they are dominating the radar resolution volume. Around 2 km, it can be seen that there is a small spike in Z_{dr} and L values drop to a small extent. This might correspond to a region of secondary ice nucleation [20].

From this case study, we can see that we can use the data collected in the ICE-POP field campaign to improve understanding of precipitation microphysics. Data from many additional snow events can be used to study the variation of the hydrometeor during different storms and time scales. In addition, data from multiple instruments can be used together for better understanding, which is discussed later in this article.

V. Dual-Frequency Ratio for Studying Snow Microphysics

In D3R, the Ku and Ka band radars both have colocated antennas mounted on the same positioner. This configuration will allow the radar to scan the same resolution volume at Ku and Ka bands. This integrated system has the added advantage of

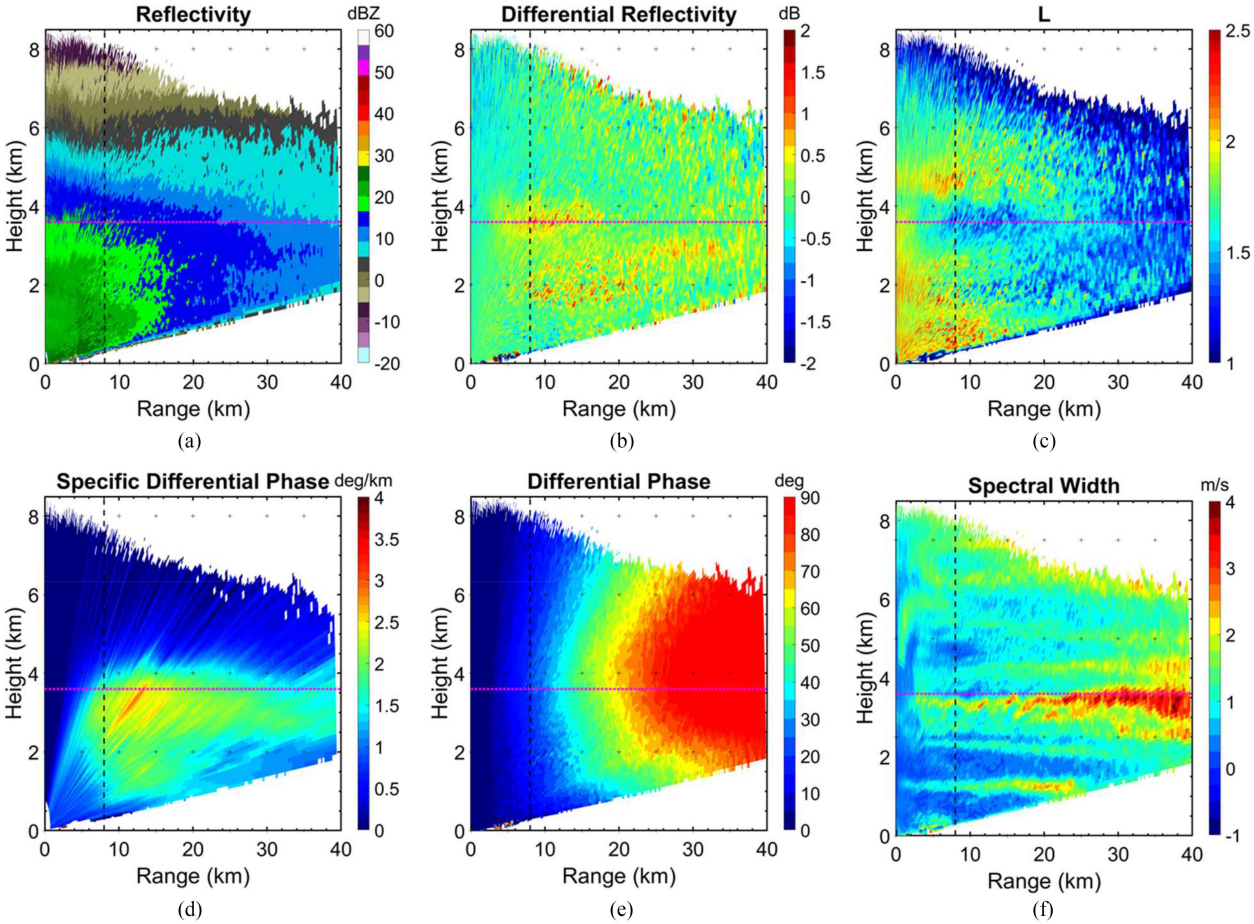

Fig. 6. Various radar moments of an RHI scan taken on the 28th of February 2018 at 06:02 UTC. (a) Reflectivity. (b) Differential reflectivity. (c) *L*. (d) Specific differential phase. (e) Differential phase. (f) Spectral width. The horizontal dotted purple line corresponds to the −15 °C isotherm. The black dashed line corresponds to the vertical profile considered in Fig 7.

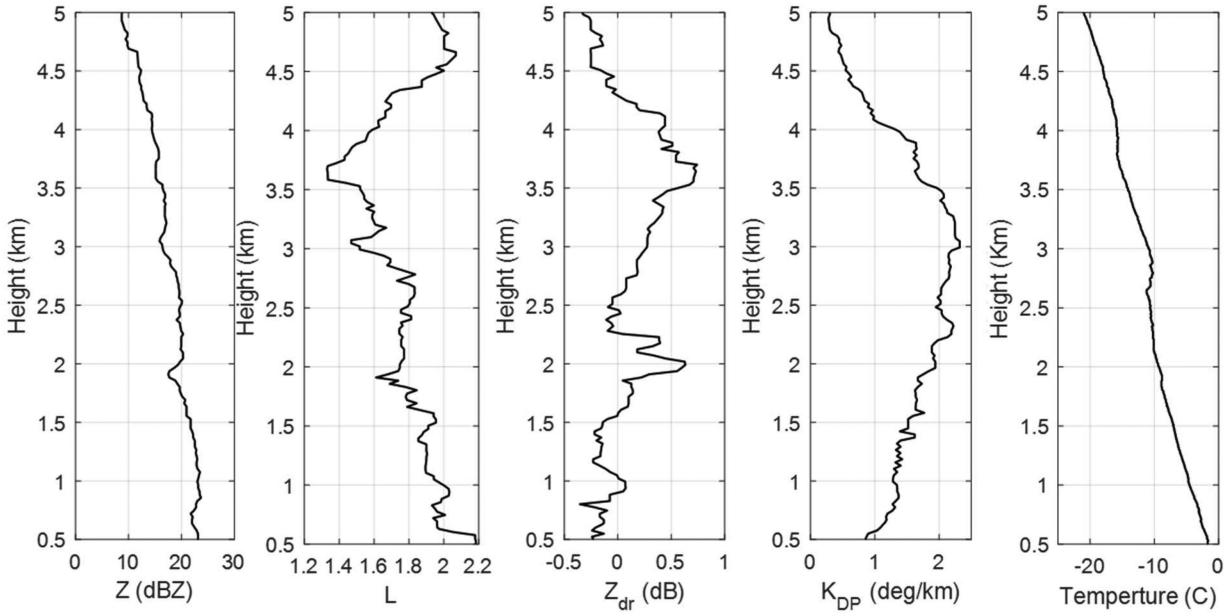

Fig. 7. Vertical profile plots at 8 km in range for the data case considered in Fig. 6.

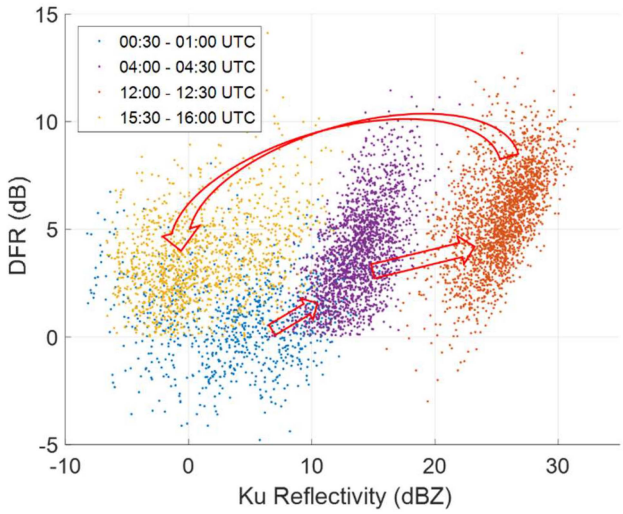

Fig. 8. D3R Ku reflectivity versus DFR for precipitation event data from D3R on the 28th of February 2018.

computing derived moments from the combination of frequencies, such as the DFR. The DFR is defined as the ratio between the equivalent radar reflectivity Z_e at two frequencies f_1 and f_2 and is given in (2).

$$\text{DFR} = \frac{Z_{f_1}}{Z_{f_2}}. \tag{2}$$

In the logarithmic scale, it is the difference between the equivalent radar reflectivity Z_e at two frequencies f_1 and f_2 [DFR $(dB) = Z_{f_1}(dBZ) - Z_{f_2}(dBZ)$]. The equivalent radar reflectivity is referred to as reflectivity further in this article. For computing DFR for D3R, f_1 is Ku band and f_2 is Ka band in (2).

We can use the information of the DFR between the Ku and Ka bands to improve the SR estimation. In [21], a detailed description of deriving a relationship for SR using the DFR and radar reflectivity is provided. In short, it is observed that using DFR in addition to radar reflectivity gives more accurate estimates of SR compared to the SR computed only using reflectivity.

Since the radar backscatter lies in the Rayleigh scattering region at the Ku band and in the Mie scattering region at Ka band, the DFR provides useful information to interpret different signatures from precipitation particles in the observation volume of a radar [22], including the capability to distinguish between rain and snow [23]. The DFR can also be used to identify changes in precipitation phases during a snowstorm.

A case study examining the influence of DFR on different precipitation particle types is discussed next. Fig. 8 shows four sets of Ku reflectivity versus DFR data from the snowstorm on the 28th of February 2018. The storm on this day lasted for several hours with varying precipitation particle types. Near vertical pointing data, which lie below 1 km in height and elevation angles from 85° to 90° from RHI scans, are considered for constructing the data points. This gives us close to vertical pointing data, which is required for the study. The time period for each set of data is 30 min. From the plot of D3R Ku reflectivity versus DFR, as shown in Fig. 8, it can be seen that for the first set of data from 00:30 to 01:00 UTC (light blue color), the DFR values are concentrated around −0.5 dB, the Ku reflectivity values were below 12 dBZ, and the temperature was below 0 °C in the region of data considered. These data points correspond to the mixed phase of the precipitation particles at the initial phase of the storm and may correspond to the presence of freezing rain particles. As the storm progressed, for the data points considered during 04:00 to 04:30 UTC (purple color), the DFR values were concentrated around 4–5 dB. The data were during the developing stage of the severe snowfall event. This might correspond to the snow aggregation increasing, similar to the DFR case studies in [23]. It was also observed from signal simulations that as the axis ratio of the particles increases, the DFR also increases. The next set of data is taken from 12:00 to 12:30 UTC (orange color). From this data, it can be seen that the DFR is concentrated around 6–7 dB. This timeframe was one of the peak snowfall durations. Since the large DFR values correspond to particles becoming more spherical due to large aggregates [24], the DFR values during this phase indicate large snow aggregates present. Finally, for the data points between 15:30 and 16:00 UTC (yellow color), the mean DFR value is around 3 dB, this was during the weakening stage of the storm, and the precipitation particles do not feature high DFR values. From this case study, we can see that the DFR values can be used to identify different ice hydrometeor types and also to interpret the various stages during the precipitation event.

VI. Comparison With Other Instruments in ICE-POP Campaign

Various instruments were deployed in addition to the D3R in the ICE-POP field campaign. This instrument network included upper air observations, surface remote sensing instruments, and instruments to measure the microphysics of precipitation [25]. Having such a wide variety of instruments deployed will be useful in understanding the precipitation evolution and characteristics in the complex terrain around PyeongChang. The instruments were placed in a network of sites known as super sites, which were chosen such that the instruments could map the atmospheric flows effectively. More details about the various equipment deployment can be found in the ICE-POP experiment document [26]. Data from some of the instruments, such as the Parsivel disdrometer, precipitation gauge, and sounding used in this study, along with D3R, were described previously. In this section, data from an X-band radar are discussed to show the potential of using D3R data along with other instruments for microphysical analysis and study.

The MXPoL X-band polarimetric radar was also deployed in the ICE-POP field campaign. This radar was located at the Gangneung-Wonju National University campus, which is about 16.9 km from DGW, where D3R was deployed. Additional details regarding the MXPoL radar and its performance during the ICE-POP campaign can be found in [27]. Fig. 9(a) shows the common volume region between D3R and MXPoL. The common volume for PPI scans lies between 5 and 7 km in range

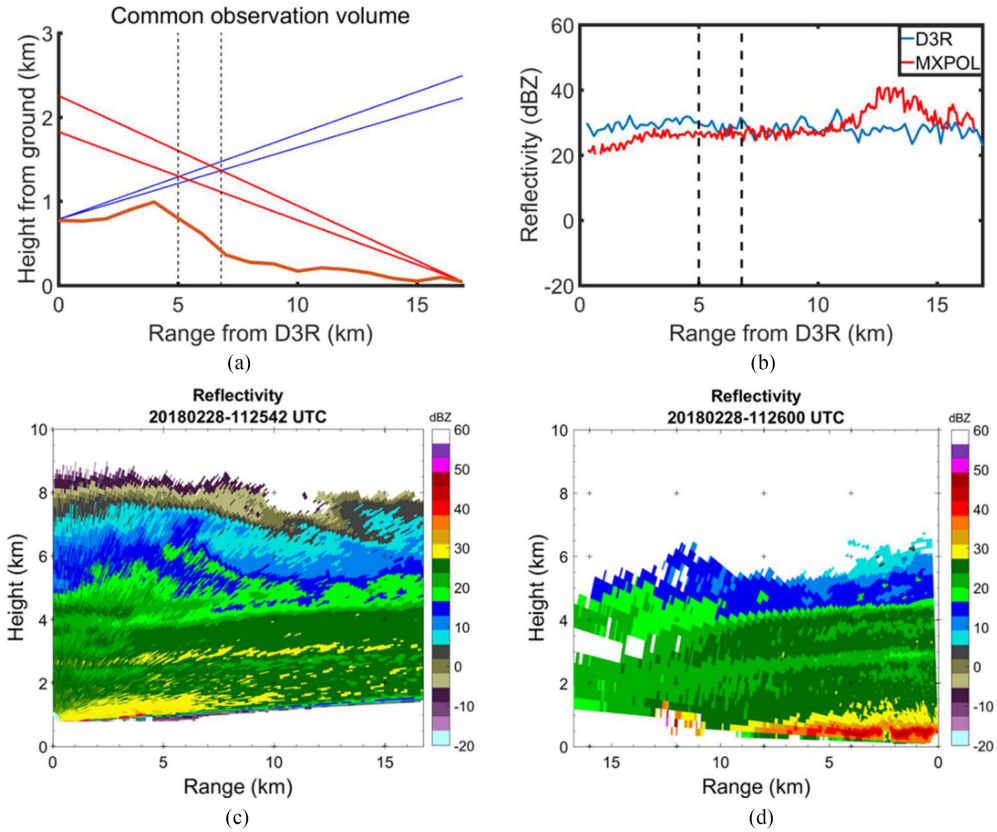

Fig. 9. D3R data comparison with MXPol X-band radar data. (a) Common observation volume between D3R and MXPol. (b) Reflectivity line plot along the common observation volume. (c) RHI plot of reflectivity from D3R. (d) RHI plot of reflectivity from MXPol radar.

from D3R when MXPoL is scanning at 6° elevation, and D3R is scanning at 4.8° elevation. In this figure, the elevation profile between D3R and MXPoL is also shown in brown color. The D3R is located at an elevation of about 785 m from sea level in the mountain ranges, and MXPOL is located at 66 m from sea level, which is in Gangneung city. It can also be seen in the figure that some of the lower scan angles of D3R and MXPOL will be blocked due to mountains. Fig. 9(b) shows the reflectivity comparison from D3R Ku band radar and MXPOL radar from a PPI scan taken on the 28th of February 2018 at 12:37 UTC. The azimuth angle with the line of sight for D3R is approximately 53° and for MXPOL is 233°. From this figure, it can be seen that the reflectivities from D3R Ku and MXPOL radars match well in the common volume region.

As mentioned before, since these two radars are located at different altitudes, the data from the radars could be used to study the cloud formation due to the ocean and mountain interface. The RHI scans from D3R and MXPoL radars taken on the 28th of February 2018 at 11:25 UTC are shown in Fig. 9(c) and (d). The RHI scans considered from the radars are looking at each other. These plots are adjusted for the altitude of the radar location. We can see from the plots that the MXPoL radar has a bright band around 0.5 km, which could not be detected from D3R because of beam blockage and the MXPoL radar sensitivity is too low to detect ice particles at 8 km in height which D3R is able to capture. It can also be seen from the figures that the minimum reflectivity that D3R could detect is around −10 dBZ. Utilizing data from both radars could help in understanding precipitation characteristics better.

VII. Summary

The NASA D3R weather radar was deployed in the PyeongChang region in South Korea for the ICE-POP 2018 field campaign. Operating at the Ku and Ka frequency bands and having a matched beam scanning system, the D3R served as a useful tool for understanding the microphysical process of snow storms. The radar systems were well calibrated, and the D3R was deployed in late October 2017 at the DGW site. The uncertainty in the measured power was within 0.5 dB. The differential reflectivity and co-polar correlation obtained from the vertical pointing D3R data are in good agreement between Ku and Ka bands. During the campaign, D3R captured many interesting rain and snow events. Data from 20 precipitation days were collected, as listed in Table I. Along with PPI scans, the radar also collected RHI scan data which gives us information on the vertical structure of the precipitation event. The radar data helped the local forecasters to monitor and predict snow events.

The relationship between the radar reflectivity and SR is provided for the D3R radar. The D3R having an unambiguous range of 40 km could be used to estimate accumulation over a large area. It was seen that accumulation from D3R, when

TABLE I
SUMMARY OF EVENTS CAPTURED BY D3R IN ICE-POP FIELD CAMPAIGN

Date	Summary
11/01/2017	Stratiform rain event concentrated in southwest region from radar
11/03/2017	Stratiform rain event within 30 km from radar
11/10/2017	Rain event within 25 km from radar
11/22/2017	Light snow within 10 km from radar
11/25/2017	Rain and snow, mixed phase event mainly on the west side of the radar
12/03/2017	Rain and snow, mixed phase event confined below 2 km in height
12/11/2017	Light snow, shallow mixed phase even
12/17/2017	Snow event within 20 km of radar range, concentrated below 2 km in height
12/23/2017	Snow event, going up to 6 km in height
12/24/2017	Snow event, going up to 6 km in height
12/30/2017	Snow event within 10 km of radar range and concentrated in northeast of radar's range. Shallow event below 3 km in height
01/07/2018	Snow clouds detected in and around radar site, super frozen clouds between 2 km and 6 km in height
01/08/2018	Notable event observed within 20 km of radar range in the northwest region confined below 1.5 km in height
01/16/2018	Snow event observed in southwest region from radar confined below 6 km in height
02/13/2018	Light snow within 15 km from radar, shallow event below 2km in height
02/14/2018	Light snow confined below 2 km in height
02/23/2018	Light snow mostly on the west of radar confined below 3 km in height
02/28/2018	Event with change in precipitation phases from cloud to rain then to snow. Massivesnow storm with more than 40 cm of snow accumulation and the storm extending up to 6 km in height
03/04/2018	Snow storm coming from the east, massivesnow event extending up to 6 km in vertical profile. More than 20 cm of snow accumulation
03/07/2018	Huge snow storm throughout South Korea, echoes moving into the radar's range from the southwest. Snow event with more than 12 cm of snow accumulation

compared to a precipitation gauge, matched very well. Due to the complex terrain around the radar, the data of the snow events collected from D3R are interesting to study the development and progress of the event. It is useful to analyze the microphysics of snow events captured during the campaign. A major snow event with a large amount of accumulation occurred on the 28th of February 2018. Data from this day are considered in this article for discussion. Vertical profile analysis was briefly discussed for one of the snapshots during the snowstorm. For this case study, radar moments and derived products, such as specific phase from D3R, were used to identify the presence of pristine oriented ice crystals along with aggregates. The temperature obtained from a colocated sounding instrument was around -15 °C at the heights where pristine crystals were present. The detection of different ice hydrometeors was also briefly introduced.

A short discussion on using the DFR from D3R for the snow event observed during the ICE-POP campaign was given. Four phases of the precipitation event were distinguished based on the DFR values obtained from vertical pointing D3R Ku and Ka data. Along with D3R, various other instruments were deployed in the ICE-POP campaign. The data from multiple instruments can be used to understand the precipitation process and microphysics of snow storms better. The comparisons from an X-band MXPOL radar with D3R data showed a good agreement in reflectivity values in the common volume region between the two radars. Overall, the D3R radar collected quality data during the ICE-POP field campaign, and this data could be used in further studies of winter precipitation.

ACKNOWLEDGMENT

The authors would like to thank the participants of the World Weather Research Program Research Development Project and Forecast Demonstration Project, International Collaborative Experiments for PyeongChang 2018 Olympic and Paralympic winter games (ICE-POP 2018), hosted by the Korea Meteorological Administration. They would also like to thank the large contribution of W. Petersen, M. Vega, M. Kumar, I. Arias, A. Morin, and J. Kim during the ICE-POP campaign, and special thanks to Dr. K. Ahn for extensive help to the D3R staff in South Korea. The authors would like to acknowledge Korean Meteorological Administration for providing data of instruments deployed during the ICE-POP campaign.

REFERENCES

[1] V. Chandrasekar, M. A. Vega, S. Joshil, M. Kumar, D. Wolff, and W. Petersen, "Deployment and performance of the Nasa D3R during the ICEPOP 2018 field campaign in South Korea," in *Proc. IEEE Int. Geosci. Remote Sens. Symp.*, 2018, pp. 8349–8351, doi: 10.1109/IGARSS.2018.8517313.

[2] "International collaborative experiments for PyeongChang 2018 olympic and paralympic winter games (ICE-POP 2018)," Accessed: May 1, 2020. [Online]. Available: https://gpm.nasa.gov/ice-pop

[3] M. A. Vega, V. Chandrasekar, J. Carswell, R. M. Beauchamp, M. R. Schwaller, and C. Nguyen, "Salient features of the dual-frequency, dualpolarized, Doppler radar for remote sensing of precipitation," *Radio Sci.*, vol. 49, no. 11, pp. 1087–1105, 2014, doi: 10.1002/2014RS005529.

[4] S. S. Joshil, "Salient features of the D3R radar enhancements," in *Proc. 2000-2019-CSU Theses Diss.*, 2018, pp. 1–55.

[5] A. Y. Hou et al., "The global precipitation measurement mission," *Bull. Amer. Meteorol. Soc.*, vol. 95, no. 5, pp. 701–722, 2014, doi: 10.1175/BAMS-D-13-00164.1.
[6] V. Chandrasekar et al., "Observations and performance of the Nasa dual-frequency dualpolarization Doppler radar (D3R) from five years of operation," in *Proc. 32nd Gen. Assem. Sci. Symp. Int. Union Radio Sci.*, 2017, pp. 1–2, doi: 10.23919/URSIGASS.2017.8105112.
[7] S. S. Joshil and C. V. Chandrasekar, "Calibration of D3R weather radar using UAV-hosted target," *Remote Sens.*, vol. 14, no. 15, 2022, Art. no. 3534, doi: 10.3390/rs14153534.
[8] M. Kumar, S. Joshil, M. Vega, V. Chandrasekar, and J. W. Zebley, "Nasa D3R: 2.0, enhanced radar with new data and control features," in *Proc. IEEE Int. Geosci. Remote Sens. Symp.*, 2018, pp. 7978–7981, doi: 10.1109/IGARSS.2018.8517944.
[9] V. Chandrasekar, L. Baldini, N. Bharadwaj, and P. L. Smith, "Calibration procedures for global precipitation-measurement ground-validation radars," *URSI Radio Sci. Bull.*, vol. 355, pp. 45–73, 2015, doi: 10.23919/URSIRSB.2015.7909473.
[10] M. Kumar, S. S. Joshil, V. Chandrasekar, R. M. Beauchamp, M. Vega, and J. W. Zebley, "Performance trade-offs and upgrade of NASA D3R weather radar," in *Proc. IEEE Int. Geosci. Remote Sens. Symp.*, 2017, pp. 5260–5263, doi: 10.1109/IGARSS.2017.8128188.
[11] E. Gorgucci, G. Scarchilli, and V. Chandrasekar, "A procedure to calibrate multiparameter weather radar using properties of the rain medium," *IEEE Trans. Geosci. Remote Sens.*, vol. 37, no. 1, pp. 269–276, Jan. 1999, doi: 10.1109/36.739161.
[12] G.-J. Huang, V. N. Bringi, D. Moisseev, W. A. Petersen, L. Bliven, and D. Hudak, "Use of 2D-video disdrometer to derive mean density–size and Ze–SR relations: Four snow cases from the light precipitation validation experiment," *Atmos. Res.*, vol. 153, pp. 34–48, 2015, doi: 10.1016/j.atmosres.2014.07.013.
[13] A. J. Heymsfield, A. Bansemer, C. Schmitt, C. Twohy, and M. R. Poellot, "Effective ice particle densities derived from aircraft data," *J. Atmos. Sci.*, vol. 61, no. 9, pp. 982–1003, 2004, doi: 10.1175/1520-0469(2004)061<0982:EIPDDF>2.0.CO;2.
[14] E. A. Brandes, K. Ikeda, G. Zhang, M. Schonhuber, and R. M. Rasmussen, "A statistical and physical description of hydrometeor distributions in Colorado snowstorms using a video disdrometer," *J. Appl. Meteorol. Climatol.*, vol. 46, no. 5, pp. 634–650, 2007, doi: 10.1175/JAM2489.1.
[15] T. Yu, V. Chandrasekar, H. Xiao, and S. S. Joshil, "Characteristics of snow particle size distribution in the PyeongChang Region of South Korea," *Atmosphere*, vol. 11, no. 10, 2020, Art. no. 1093, doi: 10.3390/atmos11101093.
[16] A. von Lerber, "Challenges in measuring winter precipitation: Advances in combining microwave remote sensing and surface observations," Aalto Univ., Espoo, Finland, 2018.
[17] W. J. Keat and C. D. Westbrook, "Revealing layers of pristine oriented crystals embedded within deep ice clouds using differential reflectivity and the copolar correlation coefficient," *J. Geophysical Res., Atmos.*, vol. 122, no. 21, pp. 11737–11759, 2017, doi: 10.1002/2017JD026754.
[18] P. C. Kennedy and S. A. Rutledge, "S-band dual-polarization radar observations of winter storms," *J. Appl. Meteorol. Climatol.*, vol. 50, no. 4, pp. 844–858, 2011, doi: 10.1175/2010JAMC2558.1.
[19] R. Bechini, L. Baldini, and V. Chandrasekar, "Polarimetric radar observations in the ice region of precipitating clouds at c-band and x-band radar frequencies," *J. Appl. Meteorol. Climatol.*, vol. 52, no. 5, pp. 1147–1169, 2013, doi: 10.1175/JAMC-D-12-055.1.
[20] P. R. Field et al., "Secondary ice production: Current state of the science and recommendations for the future," *Meteorol. Monogr.*, vol. 58, pp. 7.1–7.20, 2017, doi: 10.1175/AMSMONOGRAPHS-D-16-0014.1.
[21] T. Yu, V. Chandrasekar, H. Xiao, and S. S. Joshil, "Snowfall estimation using dual-wavelength radar during ICE-POP," *J. Meteorol. Soc. Jpn.*, vol. 99, pp. 67–77, 2020, doi: 10.2151/jmsj.2021-004.
[22] J. Tyynela and V. Chandrasekar, "Characterizing falling snow using multi-frequency dual-polarization measurements," *J. Geophysical Res., Atmos.*, vol. 119, no. 13, pp. 8268–8283, 2014, doi: 10.1002/2013JD021369.
[23] L. Liao and R. Meneghini, "A study on the feasibility of dual-wavelength radar for identification of hydrometeor phases," *J. Appl. Meteorol. Climatol.*, vol. 50, no. 2, pp. 449–456, 2011, doi: 10.1175/2010JAMC2499.1.
[24] S. Y. Matrosov, M. Maahn, and G. D. Boer, "Observational and modeling study of ice hydrometeor radar dual-wavelength ratios," *J. Appl. Meteorol. Climatol.*, vol. 58, no. 9, pp. 2005–2017, 2019, doi: 10.1175/JAMC-D-19-0018.1.
[25] G. Lee and K. Kim, "International collaborative experiments for PyeongChang 2018 Olympic and Paralympic winter games (ICE-POP 2018)," in *Proc. AGU Fall Meeting Abstr.*, 2019, vol. 2019, pp. A52B–A506.
[26] "ICE-POP instruments," Accessed: May 1, 2022. [Online]. Available: https://ghrc.nsstc.nasa.gov/home/field-campaigns/ice-pop/instruments
[27] J. Gehring et al., "Radar and ground-level measurements of precipitation collected by EPFL during the ICEPOP 2018 campaign in South-Korea," *Earth Syst. Sci. Data Discuss.*, vol. 13, pp. 417–433, 2020, doi: 10.5194/essd-13-417-2021.

Shashank S. Joshil (Student Member, IEEE) received the B.E. degree in electronics and communication engineering from Visveswaraya Technological University, Karnataka, India, in 2013, and the M.S. degree in electrical engineering in 2018 from Colorado State University, Fort Collins, CO, USA, where he is currently working toward the Ph.D. degree in electrical engineering with the Radar Group.

He had a graduate fellowship from NASA Jet Propulsion Laboratories in 2020 and 2021–2022. His research interests include the areas of radar signal processing, radar simulations, synthetic aperture radars, digital signal and image processing, and atmospheric science.

V. Chandrasekar (Fellow, IEEE) received the bachelor's degree in electrical engineering from IIT Kharagpur, Kharagpur, India, and the Ph.D. degree in electrical engineering from Colorado State University (CSU), Fort Collins, CO, USA, in 1986.

He is currently a University Distinguished Professor with CSU. He has been actively involved with research and application of ground- and space-borne weather radar systems. He has coauthored 2 textbooks, 5 general books, and more than 250 journal articles.

Prof. Chandrasekar is an Elected Fellow of AGU, the International Union of Radio Science (URSI), NOAA/CIRA, and the American Meteorological Society. He served as the Editor-in-Chief for the *Journal of Atmospheric and Oceanic Technology* and as the International Chair for Commission F URSI. He was a recipient of numerous awards, including the NASA Technical Contribution Award, the NASA Group Achievement Award, the NASA Robert H. Goddard Exceptional Achievement Award, the Outstanding Advisor Award, the CSU Innovations Award, the IEEE GRSS Distinguished Achievement Award and the Education Award, the NOAA/NWS Directors Medal of Excellence, and the Knight of the Government of Finland. He served as the General Chair for the IEEE IGARSS'06 Symposium.

David B. Wolff received the B.S. and M.S. degrees in meteorology from Texas A&M University, College Station, TX, USA, in 1986 and 1988, respectively.

He was the Science Systems and Applications, Inc., Program Manager for the Tropical Rainfall Measuring Mission ground validation (GV) program with NASA Goddard Space Flight Center. He is currently the Global Precipitation Measurement GV System Manager and GPM Deputy Project Scientist for GV.